 Related Commentary, page 1702

HIF-1α expression regulates the bactericidal capacity of phagocytes

Carole Peyssonnaux,[1] Vivekanand Datta,[2] Thorsten Cramer,[1] Andrew Doedens,[1] Emmanuel A. Theodorakis,[3] Richard L. Gallo,[2,4] Nancy Hurtado-Ziola,[4] Victor Nizet,[2] and Randall S. Johnson[1]

[1]Division of Biological Sciences, [2]Department of Pediatrics, [3]Department of Chemistry and Biochemistry, and [4]Department of Medicine, University of California, San Diego, La Jolla, California, USA.

Hypoxia is a characteristic feature of the tissue microenvironment during bacterial infection. Here we report on our use of conditional gene targeting to examine the contribution of hypoxia-inducible factor 1, α subunit (HIF-1α) to myeloid cell innate immune function. HIF-1α was induced by bacterial infection, even under normoxia, and regulated the production of key immune effector molecules, including granule proteases, antimicrobial peptides, nitric oxide, and TNF-α. Mice lacking HIF-1α in their myeloid cell lineage showed decreased bactericidal activity and failed to restrict systemic spread of infection from an initial tissue focus. Conversely, activation of the HIF-1α pathway through deletion of von Hippel–Lindau tumor-suppressor protein or pharmacologic inducers supported myeloid cell production of defense factors and improved bactericidal capacity. HIF-1α control of myeloid cell activity in infected tissues could represent a novel therapeutic target for enhancing host defense.

Introduction

The eradication of invading microorganisms depends initially on innate immune mechanisms that preexist in all individuals and act within minutes of infection. Phagocytic cell types, including macrophages and neutrophils, play a key role in innate immunity because they can recognize, ingest, and destroy many pathogens without the aid of an adaptive immune response. The effectiveness of myeloid cells in innate defense reflects their capacity to function in low-oxygen environments. Whereas in healthy tissues oxygen tension is generally 20–70 mm Hg (i.e., 2.5–9% oxygen), much lower levels (< 1% oxygen) have been described in wounds and necrotic tissue foci (1–3).

The adaptive response of mammalian cells to the stress of oxygen depletion is coordinated by the action of hypoxia-inducible transcription factor 1 (HIF-1). HIF-1 is a heterodimer whose expression is regulated by oxygen at the protein level. The protein stability of the α subunit (HIF-1α) is regulated by a family of prolyl hydroxylases. This process is directed by the interaction of HIF-1α with the von Hippel–Lindau tumor-suppressor protein (vHL). Under hypoxia, prolyl hydroxylase activity is inhibited, and HIF-1α accumulates and translocates into the nucleus, where it binds to HIF-1β, constitutively expressed. The heterodimer HIF-1 binds to the hypoxic response elements (HREs) of target gene regulatory sequences, resulting in the transcription of genes implicated in the control of metabolism and angiogenesis as well as apoptosis and cellular stress (4). Some of these direct target genes include glucose transporters, glycolytic enzymes, erythropoietin, and the angiogenic factor VEGF. Two additional HIF subunits have subsequently been cloned and named HIF-2 (5–7) and HIF-3 (8), but their regulation is less well understood.

Confirmation that HIF-1α was expressed in activated macrophages (9, 10) led us to explore the function of this transcription factor in the myeloid cell lineage. Employing conditional gene targeting, we recently showed that HIF-1α control of the metabolic shift to glycolysis plays an important role in myeloid cell–mediated inflammatory responses (11). These studies also provided preliminary in vitro evidence that deletion of HIF-1α could impair myeloid cell bactericidal activity. The effectiveness of neutrophils and macrophages in innate antibacterial defense reflects a diverse array of highly specialized cellular functions including phagocytic uptake of the bacterium, production of reactive oxygen species, activation of iNOS, and release of antimicrobial peptides (e.g., cathelicidins, defensins) and granule proteases (e.g., elastase, cathepsin). Here we perform a detailed analysis of the underlying mechanisms by which HIF-1α transcriptional control pathways contribute to the antibacterial function of myeloid cells, and for the first time, to our knowledge, determine the requirement of HIF-1α expression for myeloid cell–mediated innate immune defense in vivo. Our results indicate a pivotal role for HIF-1α in myeloid cell biology under both hypoxia and normoxia and suggest that this transcription factor may represent a unique therapeutic target for boosting immune defense function in tissues compromised by bacterial infection.

Results

Bacteria induce HIF-1α expression. Invasive pyogenic bacterial skin and soft tissue infections generate localized tissue ischemia, thrombosis, and necrosis and represent a formidable test of the adaptiveness of neutrophils and macrophages in hypoxic microenvironments. In this regard, a strain of the Gram-positive pathogen group A *Streptococcus* (GAS), isolated from a patient with necrotizing fasciitis (flesh-eating disease), was chosen as the primary

Nonstandard abbreviations used: AG, 1-amino-2-hydroxyguanidine, p-toluenesulfate; $CoCl_2$, cobalt chloride; CRAMP, cathelicidin-related antimicrobial peptide; fMLP, N-formyl-methionyl-leucyl-phenylalanine; GAS, group A *Streptococcus*; HIF-1α, hypoxia-inducible factor 1, α subunit; HRE, hypoxic response element; L-Mim, L-mimosine; MRSA, methicillin-resistant *Staphylococcus aureus*; NE, neutrophil elastase; OH-pyridone, 3-hydroxy-1,2-dimethyl-4(1*H*)-pyridone; THB, Todd-Hewitt broth; vHL, von Hippel–Lindau tumor-suppressor protein.

Conflict of interest: The authors have declared that no conflict of interest exists.

Citation for this article: *J. Clin. Invest.* **115**:1806–1815 (2005). doi:10.1172/JCI23865.

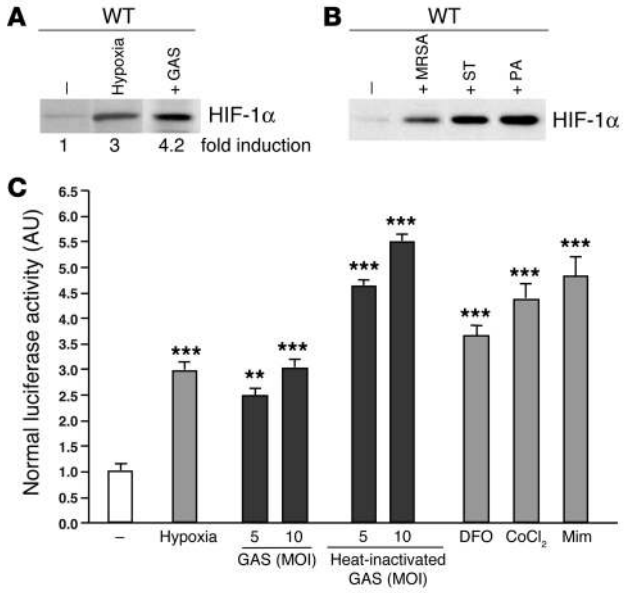

Figure 1

Bacteria increase HIF-1α protein expression and stimulate HIF-1α transcriptional activity. (**A** and **B**) Macrophages were incubated under hypoxia (0.1%) or with GAS, MRSA, *S. typhimurium* (ST), or *P. aeruginosa* (PA) at an MOI equal to 5–10 under normoxic conditions for 4 hours. Expression of HIF-1α was normalized to β-actin levels and quantified with ImageQuantTL software (Amersham Biosciences). (**C**) HRE-luciferase BM-derived macrophages were incubated either with GAS or heat-inactivated GAS at an MOI equal to 5–10 under hypoxia (1%) or with the addition of mimosine (800 μM), desferrioxamine mesylate (150 μM), or $CoCl_2$ (150 μM) for 18 hours. Statistical analyses were performed using unpaired Student's *t* test. $^{**}P < 0.01$; $^{***}P < 0.001$.

model organism for most in vitro and in vivo challenges. We found that expression of HIF-1α was increased 4-fold in WT mouse macrophages following exposure to GAS under normoxic conditions (Figure 1A). Indeed, GAS represented a more potent stimulus for HIF-1α induction than hypoxia itself. The phenomenon of bacterial induction of HIF-1α under normoxia was also observed with additional Gram-positive (methicillin-resistant *Staphylococcus aureus*, hereafter *S. aureus*) and Gram-negative (*Pseudomonas aeruginosa*, hereafter *P. aeruginosa*, and *Salmonella typhimurium*) bacterial species of medical importance (Figure 1A).

We next evaluated whether the induction of HIF-1α protein by GAS corresponded to an increase in HIF-1α transcriptional gene activation. We measured HIF-1α–dependant transcription in macrophages derived from HRE-luciferase transgenic mice, which contain a luciferase reporter gene driven by 6 consecutive specific HRE sequences. As shown in Figure 1B, a 3-fold increase in luciferase reporter activity was reached after incubating the macrophages for 18 hours in 1% oxygen or in the presence of known pharmacological inducers of HIF-1α, including desferrioxamine mesylate, cobalt chloride ($CoCl_2$), and L-mimosine (L-Mim). Incubation of the reported macrophages with live or heat-killed GAS bacteria at normoxia stimulated luciferase activity to levels comparable to or greater than those of hypoxia (Figure 1B).

HIF-1α regulates bactericidal capacity of myeloid cells. To assess the functional consequences of HIF-1α activation, we used an antibiotic protection assay to calculate intracellular killing of GAS by WT macrophages compared with killing by those derived from the bone marrow of HIF1α-lysMcre mice (11). Here, targeted deletion of the HIF-1α gene has been created via crosses into a background of cre expression driven by the lysozyme M promoter (lysMcre), allowing specific deletion of the transcription factor in the myeloid lineage (11). As shown in Figure 2A, intracellular killing of GAS by WT macrophages was increased under hypoxia, providing initial indication that HIF-1α may be involved in the bactericidal process. This result was especially notable because the facultative GAS bacteria lack oxidative phosphorylation and grow more rapidly under anaerobiasis (12). We found that, compared to WT cells, macrophages from HIF-1α–null mice showed a 2-fold decrease in GAS intracellular killing under normoxia and a 3-fold decrease in GAS intracellular killing under hypoxia (Figure 2A). Time-course studies showed that the killing defect observed in HIF-1α–null macrophages increased over time, such that 15-fold more viable bacteria were present within HIF-1α deleted cells by the last time point of 120 minutes (Figure 2B). Macrophage killing of the Gram-negative bacterium *P. aeruginosa* was likewise impaired upon deletion of HIF-1α (Figure 2B).

As a complementary analysis of the linkage of myeloid cell bactericidal functions with HIF-1α transcriptional control, we explored the effects of increased HIF-1α activity on bacterial killing by using macrophages derived from vHL-null mice. vHL is a key regulator of HIF-1α turnover; these mice have constitutively high levels of HIF-1 activity in the deleted cell population (11). We found that vHL-null macrophages showed increased intracellular killing of GAS and *P. aeruginosa* compared with WT cells across multiple time points (Figure 2C). Similar differences were observed in macrophage bactericidal assays that omitted antibiotics and instead employed vigorous washing to quantify total surviving cell-associated GAS or *P. aeruginosa* (not shown). Macrophage populations isolated from WT, HIF-1α–null, and vHL-null mice both included more than 99.5% differentiated macrophages by flow cytometric analysis, and Trypan blue straining showed similar levels of macrophage viability (98–99%) throughout the GAS-killing assays (not shown). These controls suggest that there exists an intrinsic defect in the bactericidal activity of HIF-1α–null cells that cannot be attributed to differences in the purity or viability of the explanted cell populations.

Finally, we treated WT macrophages with a number of known pharmacologic inducers of HIF-1α that each act directly or indirectly to inhibit prolyl hydroxylase targeting of HIF-1α for ubiquitination. These included the iron chelator desferrioxamine, $CoCl_2$, L-Mim, and 3-hydroxy-1,2-dimethyl-4(1*H*)-pyridone (OH-pyridone) (13). The addition of each of these agents increased intracellular killing of GAS by WT macrophages (Figure 2D). Assays were performed using a concentration of each agonist and exposure time that did not affect bacterial viability (not shown).

Myeloid cell HIF-1α production is important for control of GAS infection in vivo. We chose an animal infection model of GAS-induced necrotizing soft tissue infection for directly testing myeloid cell bactericidal function in vivo. We introduced the GAS inoculum subcutaneously into a shaved area on the flank of WT and HIF-1α$^{-/-}$ male littermates and followed progression of the infection over 96 hours. We found that mice with a tissue-specific deletion of HIF-1α in macrophage and neutrophils developed significantly larger necrotic skin lesions and experienced greater weight loss than WT mice (Figure 3, A and B). Representative gross appearance of the necrotic lesions in WT and HIF-1α myeloid–null mice is shown in Figure 3C. We next asked

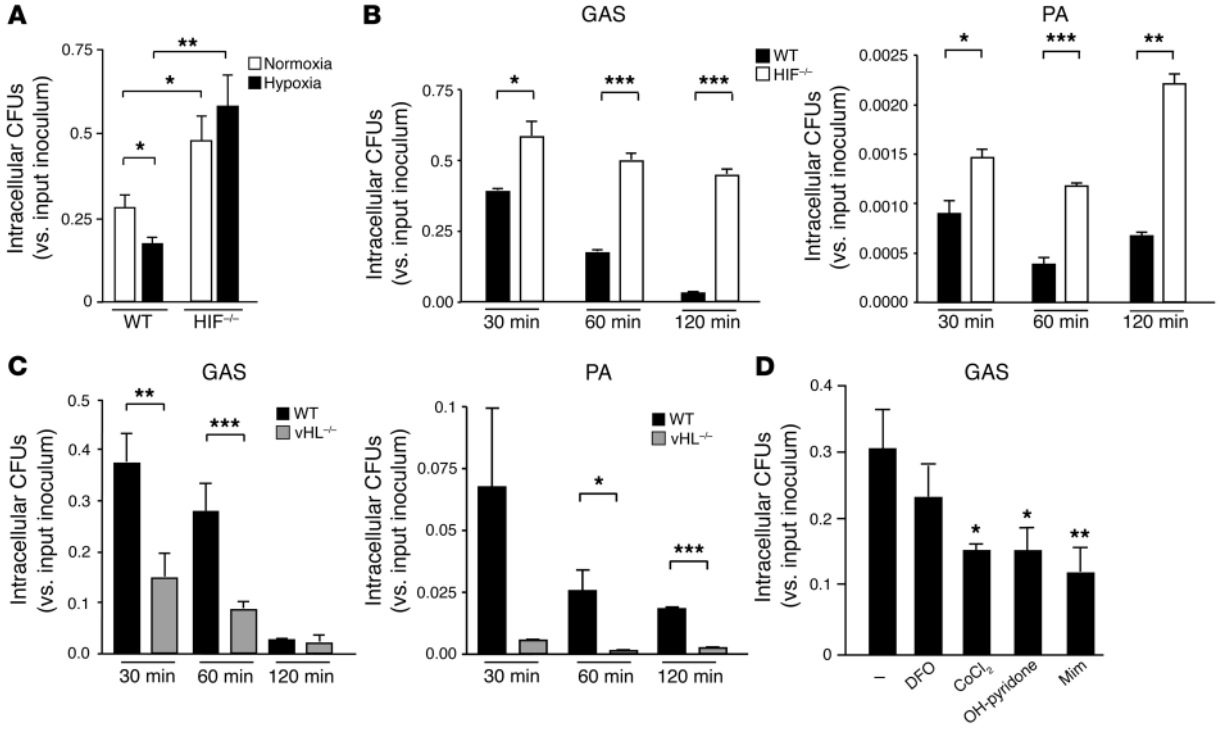

Figure 2

HIF-1α regulates bactericidal activity of myeloid cells. (**A**) Intracellular killing of GAS by WT, HIF-1α–null, or vHL-null macrophages. BM-derived macrophages were inoculated with GAS at an MOI equal to 2.5 and cultured under normoxic (white bars) or hypoxic (0.1%; black bars) conditions for 1 hour after antibiotic treatment. Statistical analyses were performed using unpaired Student's *t* test. **P* < 0.05; ***P* < 0.01. (**B**) Loss of HIF-1α in macrophages decreases intracellular killing of GAS and of *P. aeruginosa*. WT (black bars) or HIF-1α–null (white bars) BM-derived macrophages were incubated with bacteria for 1 hour before antibiotics were added. Intracellular killing was analyzed by determination of viable CFUs in macrophage lysates at the specified time points after bacterial uptake. Experiments were performed in triplicate. SEM is displayed. Experiment shown is representative of 3 repeated studies. (**C**) Loss of vHL in BM-derived macrophages increases intracellular killing of GAS and of *P. aeruginosa*. Experiments were performed in triplicate and are representative of 3 repeated studies. SEM is displayed. (**D**) Pharmacologic agonists of HIF-1α increase myeloid cell bactericidal activity. Preincubation (5 hours) with desferrioxamine mesylate (DFO), $CoCl_2$, OH-pyridone, or Mim increased the intracellular killing capacity of WT macrophages against GAS. ****P* < 0.001.

whether myeloid cell production of HIF-1α was important in limiting the ability of GAS to replicate within the necrotic skin tissues and to disseminate from the initial focus of infection into the bloodstream and systemic organs. Mice were sacrificed at 96 hours after inoculation and quantitative bacterial cultures performed on the skin ulcer (or site of inoculation if no ulcer developed), blood, and spleen (Figure 3D). Approximately 1,660-fold greater quantities of GAS were present in the skin biopsies of HIF-1α–null mice compared with those of WT mice. Similarly, 27-fold (blood) or 85-fold (spleen) more bacteria were isolated in systemic cultures from HIF-1α–null mice compared with WT mice. Our findings indicate that the presence of HIF-1α transcriptional control in neutrophils and macrophages is important in limiting the extent of necrotic tissue damage and preventing systemic spread of bacterial infection.

HIF-1α is not critical for neutrophil endothelial transcytosis or oxidative burst function. We next began a series of experiments to probe the potential cellular and molecular mechanisms through which HIF-1α may support myeloid cell functional killing capacity in vitro and in vivo. Although histopathologic examination of the biopsies from the necrotic ulcers generated by GAS revealed clear tissue ischemia by HypoxyProbe (Figure 4A), the observed immune defect of HIF-1α–null animals did not appear to reflect impaired phagocyte recruitment, since similar numbers of neutrophils were observed on immunostaining of the skin tissue of WT compared with that of HIF-1α–null mice at 6, 12, and 24 hours after infection (Figure 4B). The latter finding differed qualitatively from our previous study, in which decreased neutrophil infiltration was seen in skin tissue of HIF-1α after chemical irritation with the phorbol ester tetradecanoyl phorbol acetate (11), and from the prediction that might be derived from HIF-1α control of β2 integrin expression (14). We speculate that the stimulus to neutrophil migration elicited by bacterial infection is perhaps stronger and more complex (i.e., involving more pathways) than that of chemical irritation such that the any contribution of HIF-1α may be muted in comparison to its effects on bacterial killing. To explore further whether the migratory capacity of WT and HIF-1α–null neutrophils toward a bacterial stimulus was indeed unaffected, we measured the rate of transcytosis across murine endothelial cell monolayers following stimulation by GAS or the bacteria-derived chemotactic peptide N-formyl-methionyl-leucyl-phenylalanine (fMLP). In these assays, we also found no significant difference in transendothelial migration between the activated WT, HIF-1α–null, and vHL-null murine neutrophils (Figure 4C).

The production of reactive oxygen metabolites generated by lysosomal NADPH oxidases in a process known as the respiratory

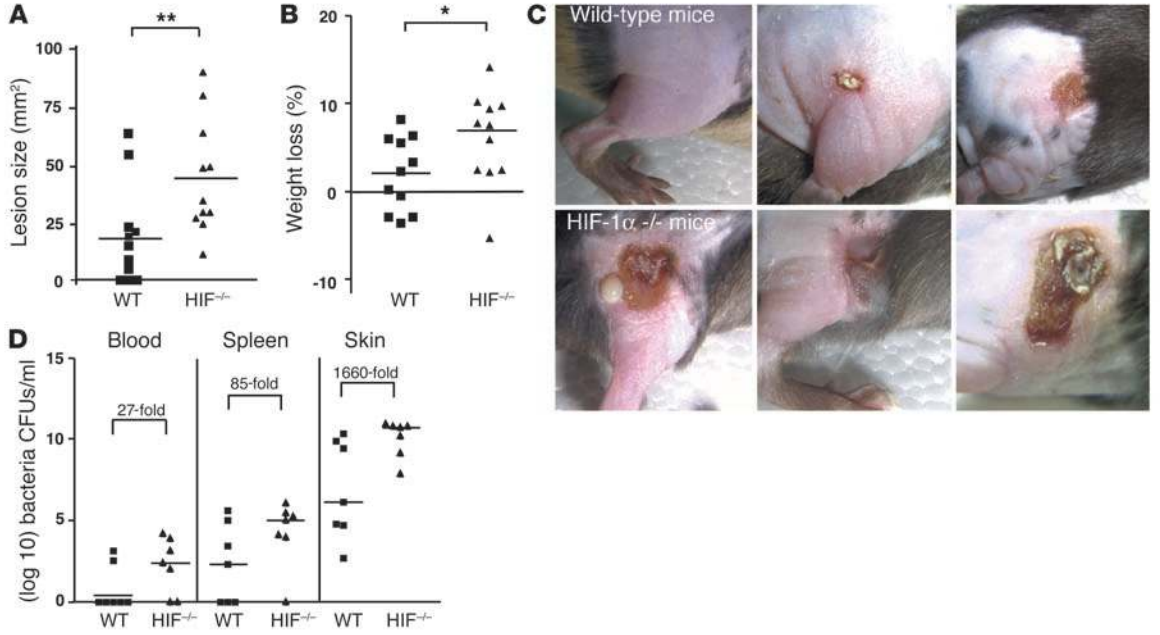

Figure 3

HIF-1α deletion renders mice more susceptible to GAS infection. (**A**) Area of necrotic ulcer and (**B**) loss of weight in individual WT (squares) and HIF-1α myeloid–null mice (triangles) 4 days after infection with GAS. (**C**) Representative appearance of GAS-induced necrotic skin ulcers in WT and HIF-1α myeloid–null mice. A total of 11 mice in each group were tested in 3 paired experiments. (**D**) Bacterial counts in the blood, spleen, and skin of WT and HIF-1α myeloid–null mice infected with GAS. The fold difference in quantitive GAS culture between WT and HIF-1α–null animals is annotated. Statistical analyses were performed using unpaired Student's *t* test. $^{*}P < 0.05$; $^{**}P < 0.01$.

burst is a major mechanism of bacterial killing. However, circulating neutrophils derived from HIF-1α–deficient or vHL-deficient mice were similar to WT neutrophils in oxidative burst activity (Figure 4D). Thus, the defect in innate immunity to GAS infection observed in HIF-1α myeloid–null mice could not be attributed to impairment in oxidative burst function.

Production of granule proteases and antimicrobial peptides is regulated by HIF-1α. Granule proteases are increasingly recognized as an important component of myeloid cell antimicrobial activity. Neutrophil elastase (NE) and cathepsin G are abundant serine proteases concentrated in the granules that are primarily destined to fuse to phagosomes and form phagolysosomes. Gene targeting of elastase in mice has directly supported a role of NE in host innate immune defense (15), and accumulating evidence suggests a similar role for cathepsin G (16–18). Patients with Chediak-Higashi syndrome lack NE and suffer recurrent bacterial infections. To determine whether HIF-1α has an impact on neutrophil production of granule proteases, we measured NE and cathepsin G activity in WT, HIF-1α–null, and vHL-null blood neutrophils. Protease activity was measured using a synthetic peptide substrate containing recognition sites for each molecule to allow either fluorometric (NE) (Figure 5A) or spectrophotometric (cathepsin G) detection (19) (Figure 5B). HIF-1α–null neutrophils showed decreased enzymatic activity of each granule protease compared with WT neutrophils while vHL-null neutrophils exhibited increased protease activity. Mixing experiments with WT and HIF-1α–null macrophages excluded the possibility that HIF-1α–null neutrophils produce a greater amount of an (unknown) inhibitor rather than less of the granule proteases (Figure 5, A and B).

The production of proteases by neutrophils may exert direct antimicrobial effects or, alternatively, may serve to activate cationic antimicrobial peptides from their inactive precursor forms (20, 21). An important component of innate immune defense in mammals is the cathelicidin family of antimicrobial peptides (22). These gene-encoded "natural antibiotics" exhibit broad-spectrum antimicrobial activity and are produced by several mammalian species on epithelial surfaces and within the granules of phagocytic cells. Proteolytic cleavage of an inactive precursor form to release the mature C terminal antimicrobial peptide is accomplished by proteases, such as elastase, upon degranulation of activated neutrophils (23). Mice have a single cathelicidin, cathelicidin-related antimicrobial peptide (CRAMP), which closely resembles the single human cathelicidin (LL-37). Importantly, we demonstrated in earlier experiments using the murine model of necrotizing skin infection that endogenous production of CRAMP was essential for mammalian innate immunity to GAS (24). We performed experiments to identify whether production or activation of CRAMP was under HIF-1α control. Lysates from WT, HIF-1α–null, and vHL-null peritoneal neutrophils were analyzed by SDS-PAGE and immunoblotted with a rabbit anti-mouse CRAMP antibody against the CRAMP mature peptide. HIF-1α deletion led to a dramatic reduction of the active mature form of cathelicidin compared with WT neutrophils while CRAMP was expressed at higher levels in vHL-deficient neutrophils (Figure 5C). Regulation of cathelicidin expression occurred at least in part at the mRNA level, as CRAMP transcript levels are reduced by 80% in HIF-1α–null macrophages, and conversely increased with loss of vHL (Figure 5D). As would be expected, CRAMP mRNA was also increased by exposure of the neutrophils to hypoxia (Figure 5D).

Thus, the production and activation of cathelicidin antimicrobial peptides represents an additional myeloid cell killing mechanism that is affected by alterations in the HIF-1α pathway.

HIF-1α is a principal regulator of NO production in response to bacterial infection. NO is known to exert antimicrobial properties against a variety of bacterial species (25). Nitric oxide is enzymatically produced by NOS through the oxidation of arginine, and mice deficient in iNOS are more susceptible to bacterial infection (26, 27). It has been well documented that HIF-1α is a transcriptional activator of iNOS expression (28–30), but no studies have examined this linkage in the context of bacterial infection. Here we found that exposure of macrophages to GAS increased iNOS mRNA production approximately 250-fold (Figure 6A). Deletion of HIF-1α resulted in an approximately 70% reduction in iNOS gene transcription, while deletion of vHL led to a marked increase in iNOS mRNA levels (Figure 6A). Measurement of nitrite in cell culture supernatants confirmed that the observed differences in iNOS induction translated directly to differences in NO production (Figure 6B). Addition of the NOS inhibitor 1-amino-2-hydroxyguanidine, p-toluenesulfate (AG) significantly inhibited the production of NO in response to GAS (Figure 6B). WT macrophages treated with L-Mim, a pharmological inducer of HIF-1α showed greatly increased expression of iNOS mRNA, but this increased expression was very low in HIF-1α–null cells (Figure 6C), confirming a dependency of the observed effect on the presence of the transcription factor. These experiments indicate that augmentation of iNOS expression and subsequent bacterial killing (Figure 2C) can be pharmacologically induced through increased HIF-1α expression.

To establish the functional importance of HIF-1α–induced iNOS expression and NO production, we performed macrophage bactericidal assays in the presence or absence of AG. Figure 6D shows that AG inhibited the bactericidal activity of WT macrophages but did not further suppress the poor bactericidal activity of HIF-1α–null macrophages. We found similar results using the iNOS-specific inhibitor 1400W (not shown). It has recently been demonstrated that NO, as well as certain reactive oxygen species, cytokines, and growth factors, can participate in stability regulation of HIF-1α and HIF-1 transactivation during normoxia (31–36). As seen in Figure 6E, we found that inhibition of iNOS by AG blocked the ability of GAS exposure to generate increased levels of HIF-1α in WT macrophages. Thus, HIF-1α induces the production of NO, which not only acts as a key element in bacterial killing, but also serves as a regulatory molecule that further stabilizes HIF-1α. This places HIF-1α at the center of an amplification loop during the innate immune response of myeloid cells to bacterial infection.

HIF1-α regulates myeloid cell TNF-α production through a NO-dependent process. We next examined the expression pattern of TNF-α, a cytokine involved in the augmentation of inflammatory responses to bacterial infection. Indeed, development of GAS-necrotizing fasciitis has been reported as a complication of anti–TNF-α therapy (37). As shown in Figure 7A, GAS strongly induced TNF-α mRNA production in WT macrophages. This transcriptional response was severely diminished in HIF-1α–null macrophages and upregulated in vHL-null macrophages. Whereas basal levels of

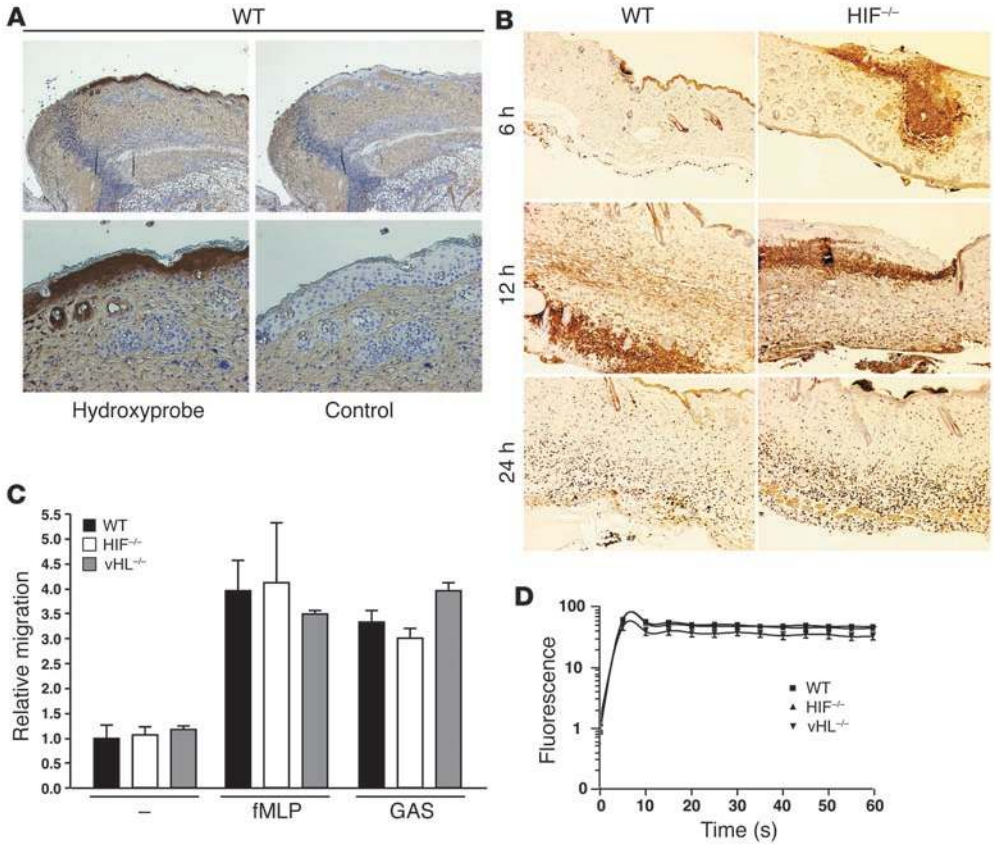

Figure 4

HIF-1α is not critical for neutrophil endothelial transcytosis or oxidative burst function. (**A**) Hypoxia is present in lesions generated by GAS infection. Immunostaining for hypoxic markers in WT mouse skin upon GAS infection. Magnification, ×100 (top); ×200 (bottom). The control corresponds to the omission of primary antibody. (**B**) Similar numbers of neutrophils in WT and HIF-1α–null mouse skin tissue observed by immunostaining at 6, 12, and 24 hours after infection. Magnification, ×100. (**C**) Migratory capacity of activated neutrophils across endothelium is not affected by the deletion of HIF-1α. Count of neutrophils transcytosing pulmonary endothelial monolayer toward GAS or fMLP stimulus is shown. (**D**) HIF-1α activity does not affect oxidative burst capacity. Flow cytometry of leukocytes derived from WT (squares), HIF-1α–null (triangles) and vHL-null (inverted triangles) mice. Oxidative burst capacity as measured by fluorescence before (0 seconds) and after the addition of a reagent designed to stimulate leukocyte phagocytic and oxidative activity as described in Methods. Data are representative of the results obtained for 4 individuals per genotype.

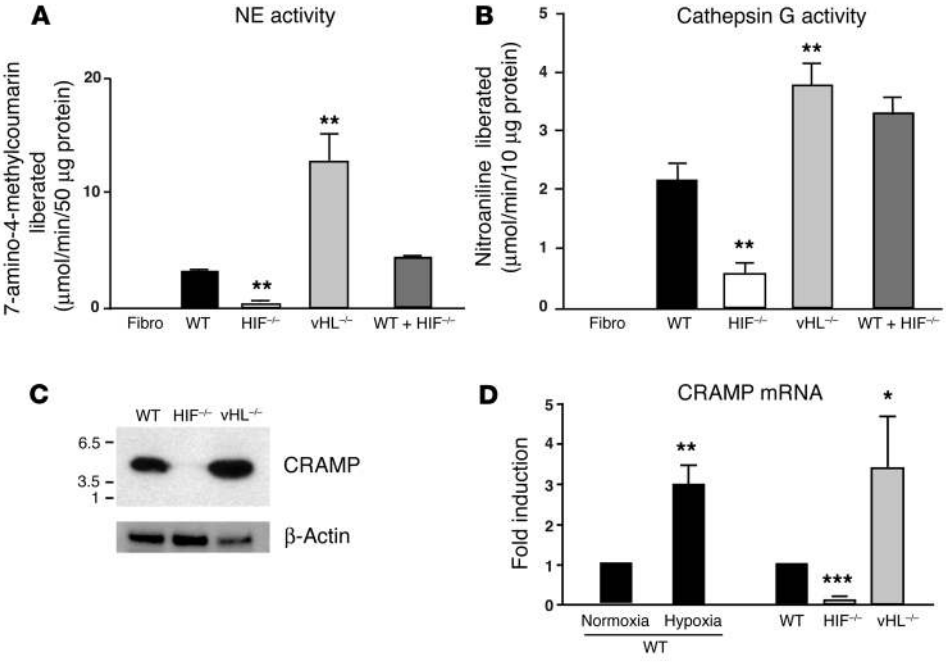

Figure 5
Production of granule proteases and of murine CRAMP is regulated by HIF-1α. NE (**A**) and cathepsin G (**B**) activity in WT, HIF-1α–null, vHL-null and in a mix of WT and HIF$^{-/-}$ blood leukocytes. (**C**) Neutrophils were processed for immunoblotting with anti-CRAMP antibody (upper panels) or anti–β-actin antibody (lower panels). (**D**) HIF-1α regulates CRAMP at the mRNA level. Neutrophils were cultured under normoxic or hypoxic (0.1%) conditions. Total neutrophil RNA was extracted and mRNA polyA$^+$ isolated by an Oligotex mRNA spin-column protocol (QIAGEN). WT neutrophils were arbitrarily set to 1 unit following normalization to β-actin RNA levels. Statistical analyses were performed using unpaired Student's *t* test. $^*P < 0.05$; $^{**}P < 0.01$; $^{***}P < 0.001$.

TNF-α protein expression were similar in WT, HIF-1α, and vHL-null macrophages, loss of HIF-1α also strongly depressed the rapid secretion of TNF-α protein in response to GAS (Figure 7B). As NO is markedly induced under GAS stimulation, TNF-α induction by GAS may rely on HIF-1α–dependent NO production. ELISA for secreted TNF-α demonstrated reduced amounts of TNF-α protein in conditioned supernatants of WT, HIF-1α, and vHL-deficient macrophages in the presence of the iNOS inhibitor AG (Figure 7B). This finding indicates that NO production, acting in a HIF-1α controlled manner, contributes significantly to the macrophage TNF-α response to bacterial infection.

Discussion

Our studies use conditional gene targeting in the myeloid cell lineage to demonstrate that HIF-1α transcriptional regulation plays an important role in innate immunity to bacterial infection. Activation of HIF-1α under hypoxia enhances bactericidal activity, and HIF-1α pathways are responsive to bacterial stimulation even under normoxia. While certain myeloid cell functions, including endothelial transmigration and respiratory burst activation, appear to be independent of HIF-1α control, the transcription factor is involved directly or indirectly in the regulation of specific immune functions including NO, granule proteases (cathepsin G, NE), and cathelicidin antimicrobial peptides. The marked reduction of granule protease and cathelicidin expression in HIF-1α–deficient neutrophils correlates with diminished bactericidal activity in vitro and failure to control infection in vivo, lending support to recent studies uncovering a key role for these neutrophil effectors in mammalian innate immunity (15, 24).

Successful control of infection in the peripheral tissues requires that host myeloid phagocytic cells function effectively in hypoxic environments. The challenge to immune defense is made more critical when the microbial toxins or local edema damage host cells and the vascular supply of oxygen to the tissues becomes further compromised. The placement of essential microbial killing functions of myeloid cells under regulation of HIF-1α therefore represents an elegant controlled-response system (Figure 8). Bactericidal mechanisms can be maintained in an "off" state while the myeloid cells circulate in the oxygen-rich bloodstream and then be activated in response to the declining oxygen gradient encountered upon diapedesis and entry of the phagocytes into the infected tissues. Additional, more potent stimulation of the HIF-1α transcriptional pathway is then provided by direct encounter with the bacteria (Figure 1A). A regulatory mechanism by which HIF-1α targets genes involved in microbial killing ensures that the corresponding inflammatory mediators are expressed preferentially in tissue foci of infection but not in healthy tissues where inflammatory damage might otherwise harm host cells.

Our experiments also reveal that NO production is a myeloid cell–killing mechanism principally regulated by HIF-1α during bacterial infection. Further, we suggest that NO is likely to play a key role in the amplification of the inflammatory response through stimulation of TNF-α release. Although the effects of inflammatory cytokines on regulating NO production have been extensively studied (38–40), the reverse relationship pertaining to the effect of NO on cytokines remains controversial (41–44). A recent study demonstrated that suppression of NO could inhibit LPS-induced TNF-α and IL-1 release and pinpointed such modulation to the pretranslational level (45). We find here that macrophage production of TNF-α is dependent on NO levels controlled in turn by HIF-1α transcriptional regulation of iNOS.

Recent data has established that HIF-1α is subjected to stability regulation by soluble intracellular messengers, such as NO and TNF-α (33, 34). With such processes at play, one can speculate that HIF1-α is situated at the center of an amplification loop mechanism for innate immune activation: stimulation of HIF-1α by oxygen depletion and bacterial exposure induces the production of NO and TNF-α, which function not only to generate inflammation and control bacterial proliferation but also as regulatory molecules to further stabilize HIF-1α in myeloid cells recruited to the infectious focus.

The relative contributions of HIF-1 and HIF-2 to the regulation of gene expression in hypoxic macrophages is still under debate.

Detectable levels of HIF-2α, but not HIF-1α, have been found in a human promonocytic cell line following hypoxic induction in vitro and in tumor-associated macrophages (46, 47). In contrast, immunoreactive HIF-1α has been detected in human macrophages in the hypoxic synovia of arthritic human joints (10), and human macrophages accumulate higher levels of HIF-1 than of HIF-2 when exposed to tumor-specific levels of hypoxia in vitro (9). Our present results also clearly support a specific and independent action of HIF-1α. Taken together, these findings suggest that HIF-1 may be the major hypoxia-inducible transcription factor in macrophages.

In summary, our results demonstrate that HIF-1α not only helps myeloid cells shift to glycolytic metabolism (11) but also functions in coordinating a proper innate immune response for bacterial killing in hypoxic microenvironments. The in vivo studies confirm that the HIF-1α pathway can play a critical role in controlling proliferation of a bacterial pathogen in compromised tissues. Recent commentaries have suggested that downregulation of HIF-1α could have a therapeutic effect in disease states characterized by chronic inflammation (48, 49). We now have shown that medically important bacterial species such as GAS, methicillin-resistant *S. aureus* (MRSA), *P. aeruginosa*, and Salmonella species can trigger HIF-1α expression. Thus, the present studies suggest that rational design of pharmaceutical HIF-1α agonists (or vHL antagonists) to boost myeloid cell microbicidal activity may likewise represent a novel approach for adjunctive therapy of complicated infections due to antibiotic-resistant pathogens or compromised host immunity.

Methods

All procedures involving animals were reviewed by the University of California San Diego Animal Care Committee, which serves to ensure that all federal guidelines concerning animal experimentation are met.

Harvest of neutrophils, macrophages, and blood leukocytes. Neutrophils were either isolated from the peritoneal cavity 3 hours after injection of thioglycollate as previously described (11, 50) or derived from bone marrow as described (51). To isolate BM-derived macrophages, the marrow of femurs and tibias of WT, HIF-1α myeloid–null, or vHL myeloid–null mice were collected. Cells were plated in DMEM supplemented with 10% heat-inactivated FBS and 30% conditioned medium (a 7-day supernatant of fibroblasts from cell line L-929 stably transfected with an M-CSF expression vector). Mature adherent BM cells were harvested by gentle scraping after 7 days in culture. To isolate blood leukocytes, 200–500 μl of whole blood was collected by retroorbital bleed into cold EDTA-coated capillary tubes (Terumo Medical Corp.). Cells were centrifuged, erythrocytes were lysed using ACK RBS lysis buffer (0.15 M NH_4Cl, 10.0 mM $KHCO_3$, 0.1 mM EDTA), and unlysed cells were washed once with 1 ml PBS 1% BSA.

Bacterial strains and media. GAS strain 5448 is an M1 serotype isolate from a patient with necrotizing fasciitis and toxic shock syndrome (52). Additional bacterial strains were obtained from the ATCC Bacteriology collection, specifically methicillin-resistant *S. aureus* (ATCC 33591, designation 328), *S. typhimurium* (ATCC 1311), and *P. aeruginosa* (ATCC 27853, designation Boston 41501). GAS was propagated in Todd-Hewitt broth (THB) (Difco; BD Diagnostics) and other strains in Luria-Bertani broth.

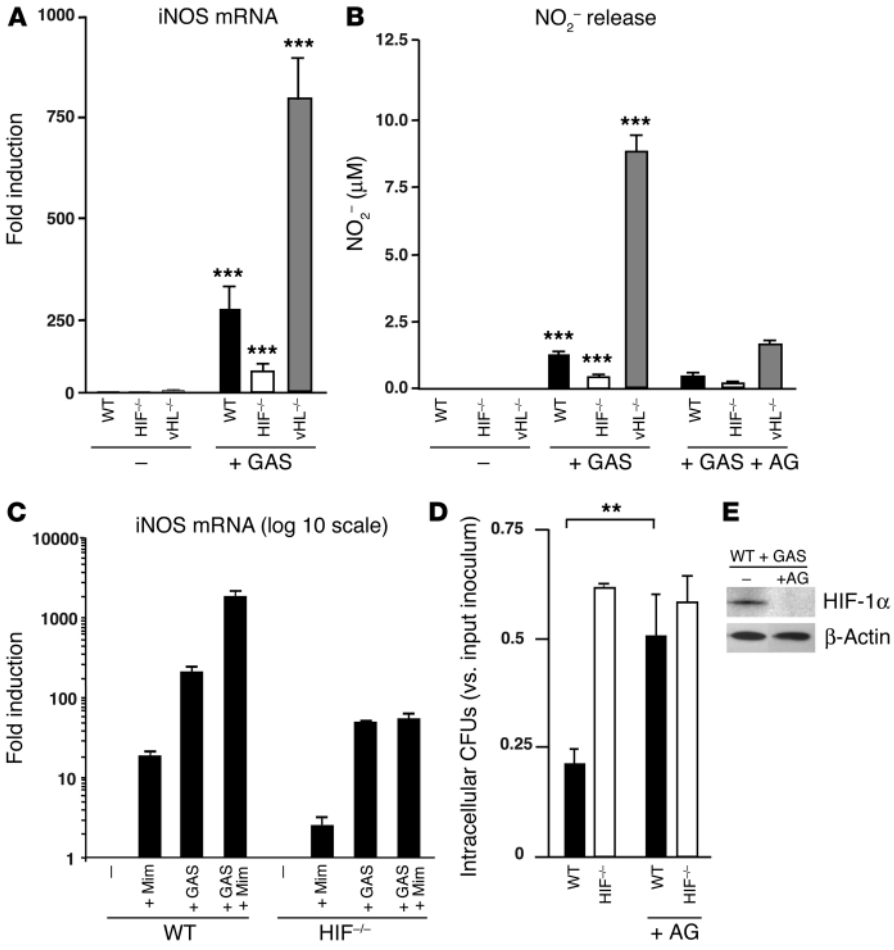

Figure 6

HIF-1α and vHL regulate NO production. (**A**) Total RNA from WT, HIF-1α$^{-/-}$, and vHL$^{-/-}$ bone marrow–derived macrophages infected with GAS isolated 3 hours after antibiotic treatment. iNOS mRNA was quantified by RT-PCR. WT, nonstimulated macrophages were arbitrarily set to 1 unit following normalization to ribosomal RNA levels. (**B**) NO production under GAS stimulation ± 1.5 mM AG (1-amino-2-hydroxyguanidine, p-toluenesulfate; Calbiochem). BM-derived macrophages were cultured for 20 hours, conditioned supernatant collected, and NO protein levels measured by the Griess assay. (**C**) Mim enhances iNOS expression of WT macrophages stimulated by GAS. Total RNA from WT and HIF-1α–null BM-derived macrophages infected with GAS ± Mim isolated 3 hours after antibiotic treatment. iNOS mRNA was quantified by RT-PCR. WT, noninfected macrophages were arbitrarily set to 1 unit following normalization to ribosomal RNA levels. Statistical analyses performed by unpaired Student's *t* test. $^{**}P < 0.01$; $^{***}P < 0.001$. (**D**) Inhibition of iNOS by AG blunts observed differences between HIF-1α–null and WT microbicidal activity. (**E**) Inhibition of iNOS prevents GAS-induced HIF-1α expression. Expression of HIF-1α is normalized to β-actin levels.

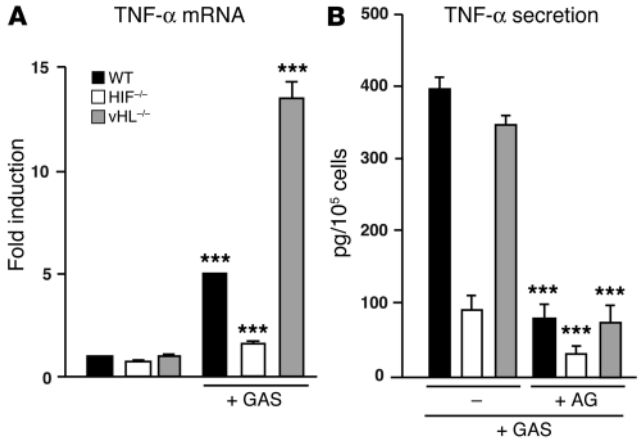

Figure 7
HIF-1α and vHL regulate TNF-α production. (**A**) Total RNA from WT, HIF-1α$^{-/-}$, and vHL$^{-/-}$ bone marrow–derived macrophages infected with GAS were isolated 3 hours after antibiotic treatment. TNF-α mRNA was quantified by RT-PCR. WT, nonstimulated macrophages were arbitrarily set to 1 unit following normalization to ribosomal RNA levels. (**B**) Inhibition of iNOS decreases TNF-α production. BM-derived macrophages were cultured for 1 hour after antibiotic treatment. Conditioned supernatant was harvested and TNF-α protein analyzed by ELISA (eBiosciences). Statistical analyses were performed using unpaired Student's *t* test. ***$P < 0.001$.

Bacterial killing assays. GAS were grown to logarithmic phase in THB to OD_{600} = 1 × 10^8 cfu/ml. Bacteria were added to macrophages at an MOI of 2.5 bacteria/cell and intracellular killing assessed using an antibiotic protection assay (11, 53) or, alternatively, total cell-associated bacteria measured by vigorous washing with PBS × 3 to remove nonadherent bacteria. At the end of the assay, total cell lysate was plated on THB agar for enumeration of CFU. Comparable studies were performed with *P. aeruginosa* at an MOI of 25. To assess macrophage viability, the monolayers were washed with PBS and incubated with 0.04% Trypan blue for 10 minutes at 37°C. As specified in the Figure 2 legend and in Results, macrophages were preincubated with L-Mim (800 μM), OH-pyridone (150 μM), desferrioxamine mesylate (100 μM), or $CoCl_2$ (100 μM) for 5 hours prior to the killing assay; each drug level was known to be sufficient for HIF-1α induction (13). Absence of bacterial inhibition was tested by incubating the drugs at the above concentrations with GAS (~10^5) at 37°C for 1–24 hours.

Mouse model of GAS infection. An established model of GAS subcutaneous infection was adapted for our studies (24, 54). Briefly, 100 μl of a midlogarithmic growth phase (~10^7 cfu) of GAS was mixed with an equal volume of sterile Cytodex beads (Sigma-Aldrich) and injected subcutaneously into a shaved area on the flank of 5- to 8-week-old male littermates. Mice were weighed daily and monitored for development of necrotic skin lesions. After 96 hours, skin lesions, spleen, and blood (via retroorbital bleeding) were collected and homogenized in 1:1 mg/ml PBS. Serial dilutions of the mixture were plated on THB agar plates for enumeration of CFUs.

Immunohistochemistry. Lesions were processed, embedded into paraffin, and routine sections (5 μm) cut. Immunohistochemistry was performed with an antibody specific for neutrophils (purified anti-mouse neutrophils mAb; Accurate Chemical & Scientific Corp.) as described (55). To assess development of hypoxic regions within the lesions, mice were injected intraperitoneally with 60 mg/kg (weight/volume in PBS) pimonidazole (Hydroxyprobe-1, Natural Pharmacia International Inc.) 2 hours prior to sacrifice. Immunohistochemistry was performed with Hydroyprobe-1 mouse monoclonal antibody as reported (56).

Reverse transcription and real-time quantitative PCR. First-strand synthesis was obtained from 1 μg of total RNA isolated with Trizol reagent (Molecular Research Center Inc.) by the SuperScript system (Invitrogen Corp.), employing random primers. For real-time PCR (RT-PCR) analyses, cDNAs were diluted to a final concentration of 10 ng/μl and amplified in a TaqMan Universal Master Mix, SYBR Green (Applied Biosystems). cDNA (50 ng) was used as a template to determine the relative amount of mRNA by RT-PCR in triplicate (ABI PRISM 7700 Sequence Detection System; Applied Biosystems), using specific primers with the following sequences: iNOS forward 5′-ACCCTAAGAGTCACAAAATGGC-3′; iNOS reverse 5′-TTGATCCTCACATACTGTGGACG-3′; TNF-α forward 5′-CCATTCCTGAGTTCTGCAAAGG-3′; TNF-α reverse 5′-AGGTAGGAAGGCCTGAGATCTTATC-3′; TNF-α probe 5′-6[FAM]AGTGGTCAGGTTGCCTCTGTCTCAGAATGA[BHQ]-3′; CRAMP forward 5′-CTTCAACCAGCAGTCCCTAGACA-3′; CRAMP reverse 5′-TCCAGGTCCAGGAGACGGTA-3′; elastase forward 5′-TGGCACCATTCTCCCGAG-

Figure 8
Model for the role of HIF-1α in myeloid cell innate immune function. Bactericidal mechanisms can be maintained in an "off" state while myeloid cells circulate in the oxygen-rich bloodstream. Transendothelial migration toward an infectious focus occurs in a HIF-1α independent fashion, but upon diapedesis, specific bactericidal mechanisms are activated through HIF-1α induction in response to the declining oxygen gradient. Further potent stimulation of the HIF-1α transcriptional pathway is provided after direct encounter with the infecting bacterial pathogen. HIF-1α regulates the generation of critical molecular effectors of immune defense, including granule proteases, antimicrobial peptides, and TNF-α. HIF-1α also stimulates the production of NO, which not only acts as an antimicrobial agent and inflammatory mediator but further amplifies myeloid cell bactericidal activity via HIF-1α stabilization.

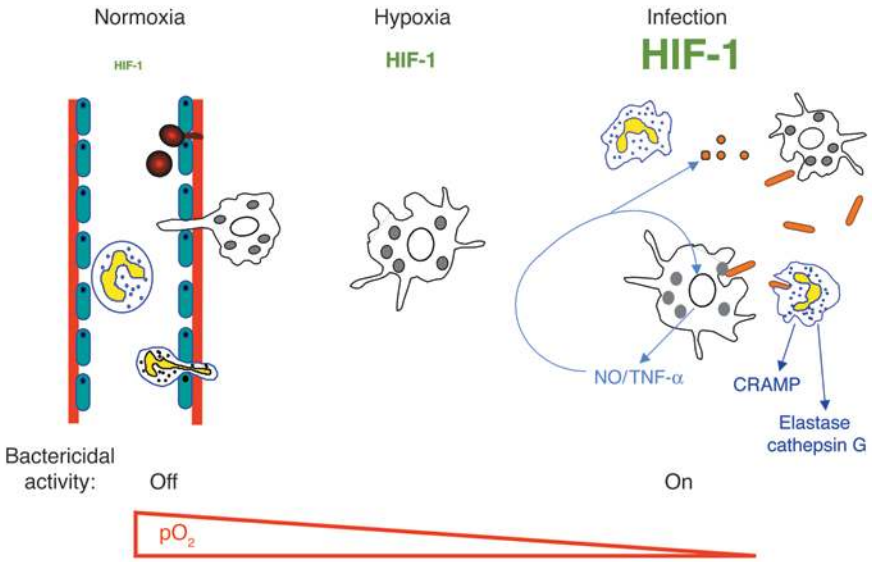

3′; elastase reverse 5′-CATAGTCCACAACCAGCAGGC-3′; β-actin forward 5′-AGGCCCAGAGCAAGAGAGG-3′; and β-actin reverse 5′-TACATGGCTGGGGTGTTGAA-3′

Nitrite determination. The concentration of nitrite (NO_2^-), the stable oxidized derivative of NO, was determined in 100-μl aliquots of cell culture supernatants transferred to 96-well plates. Essentially, 100 μl of Griess reagent (1% sulfanilamide, 0.1% naphthylene diamine dihydrochloride, 2% H_3PO_4) was added per well, and the absorbances were measured at 540 nm in a microplate reader. Sodium nitrite diluted in culture medium was used as standard.

Elastase and cathepsin G assays. For elastase measurement, 100 μl of 0.2M Tris-HCL (pH 8.5) containing 1M NaCl was mixed with 50 μg of blood leukocytes lysed in HTAB buffer containing 0.1M Tris-Cl, pH 7.6, 0.15 M NaCl, and 0.5% hexadecyltrimethylammonium bromide. Next, 100 μl of MeOSuc-Ala-Ala-Pro-ValNmec dissolved in DMSO at 20 mM was added to the buffered enzyme to start the reaction. The hydrolysis of the substrate was monitoring spectrofluorometrically using excitation at 370 nm and emission at 460 nm. For cathepsin G quantitation, 20 μl of Suc-Ala-Ala-Pro-Phe-NphNO$_2$ dissolved at 20 mM in DMSO was diluted to 180 μl with 0.1 M HEPES buffer, pH 7.5. The reaction was started by the introduction of 10 μg of blood neutrophils lysed in HTAB buffer, and the increase in A_{410} was monitored.

Western blot studies. Peritoneal neutrophils or bone marrow–derived macrophages inoculated with GAS were harvested and washed with PBS, and proteins were extracted with HTAB or RIPA buffers. Protein concentration was calculated using the Bio-Rad assay (Bio-Rad Laboratories). Fifty milligrams of protein or nuclear extracts were loaded on a 10% Tris-tricine gel in an MES buffer (Invitrogen Corp.) or 3–8% Tris-tricine gel in a Tris-acetate buffer (Invitrogen Corp.) for CRAMP and HIF-1α Western blot respectively. Proteins were transferred to a nitrocellulose membrane; the membrane was blocked in 5% nonfat milk in 0.2% Tween TBS and then incubated in primary Ab diluted in 5% nonfat milk. The primary Abs used were rabbit anti-mouse CRAMP against the CRAMP mature peptide and rabbit anti-mouse HIF-1α (Cayman Chemical Co.). The secondary Ab was peroxidase-conjugated goat anti-rabbit (DAKO Corp.). Immunoreactive proteins were detected using the ECL chemiluminescent system (Amersham Biosciences).

Reporter assay. Macrophages were derived from the marrow of femurs and tibiae of transgenic HRE-luciferase mice as described above. The luciferase reporter gene in these mice is driven by 6 specific HRE sequences. Cells were incubated with GAS or heat-inactivated GAS for 18 hours. As a positive control, macrophages were incubated under hypoxia (1%) or with the addition of L-Mim (800 μM), desferrioxamine mesylate (150 μM), or $CoCl_2$ (150 μM) during the same period of time. Cells were then washed out with PBS, and luciferase assay was performed by using the Bright-Glo Luciferase Assay kit (Promega Corp.). Luciferase activities were measured using a luminometer.

Oxidative burst assay. Isolated total blood leukocytes were resuspended at 4°C in approximately 200 μl endotoxin- and pyrogen-free PBS, lacking Ca^{2+} and Mg^{2+} but containing 5 mM glucose. Immediately before the oxidative burst assay, 200 μl of PBS at 37°C containing 1.5 mM Mg^{2+} and 1.0 mM Ca^{2+} were added to the cell suspension. Oxidative burst activity was measured by using the Fc OxyBURST Green assay reagent (Invitrogen Corp.) according to the manufacturer's instructions.

Endothelial cell transmigration assay. Thioglycolate-stimulated neutrophils were added to the upper chamber of a Transwell membrane (Corning HTS) coated with a primary murine pulmonary endothelial monolayer. The chemokine fMLP (8 ng/μl) or GAS (MOI = 10:1) was added to the lower well. The number of neutrophils migrating to the lower chamber was counted after 1 hour of incubation at 37°C.

Reagents. AG and 1400W were purchased from EMD Biosciences. L-Mim, OH-pyridone, desferrioxamine mesylate, and $CoCl_2$ were purchased from Sigma-Aldrich.

Acknowledgments

This work was supported by NIH grants CA82515 (to R.S. Johnson) and AI48694 (to V. Nizet), a La Ligue Nationale Contre le Cancer fellowship (to C. Peyssonnaux), a Deutsche Forschungsgemeinschaft fellowship (to T. Cramer), and a grant from the Edward J. Mallinckrodt, Jr. Foundation (to V. Nizet). We would like to acknowledge Kelly Doran, Ronak Beigi, Wayne McNulty, Dominique Sawka, and other members of the Johnson and Nizet laboratories for helpful suggestions and assistance.

Received for publication November 9, 2004, and accepted in revised form March 29, 2005.

Address correspondence to: Victor Nizet, Department of Pediatrics, University of California, San Diego, 9500 Gilman Drive, Mail Code 0687, La Jolla, California 92093-0687, USA. Phone: (858) 534-7408; Fax: (858) 534-5611; E-mail: vnizet@ucsd.edu. Or to: Randall S. Johnson, Molecular Biology Section, University of California, San Diego, 9500 Gilman Drive, Mail Code 0377, La Jolla, California 92093-0377, USA. Phone: (858) 822-0509; Fax: (858) 822-5833; E-mail: rsjohnson@ucsd.edu.

Thorsten Cramer's present address is: Section of Molecular Gastroenterology, Charite-Hochschulmedizin Berlin, Campus Virchow-Clinic, Berlin, Germany.

1. Vogelberg, K.H., and Konig, M. 1993. Hypoxia of diabetic feet with abnormal arterial blood flow. *Clin. Investig.* **71**:466–470.
2. Arnold, F., West, D., and Kumar, S. 1987. Wound healing: the effect of macrophage and tumour derived angiogenesis factors on skin graft vascularization. *Br. J. Exp. Pathol.* **68**:569–574.
3. Negus, R.P., Stamp, G.W., Hadley, J., and Balkwill, F.R. 1997. Quantitative assessment of the leukocyte infiltrate in ovarian cancer and its relationship to the expression of C-C chemokines. *Am. J. Pathol.* **150**:1723–1734.
4. Semenza, G.L. 2001. HIF-1 and mechanisms of hypoxia sensing. *Curr. Opin. Cell Biol.* **13**:167–171.
5. Flamme, I., et al. 1997. HRF, a putative basic helix-loop-helix-PAS-domain transcription factor is closely related to hypoxia-inducible factor-1α and developmentally expressed in blood vessels. *Mech. Dev.* **63**:51–60.
6. Ema, M., et al. 1997. A novel bHLH-PAS factor with close sequence similarity to hypoxia-inducible factor 1α regulates the VEGF expression and is potentially involved in lung and vascular development. *Proc. Natl. Acad. Sci. U. S. A.* **94**:4273–4278.
7. Tian, H., McKnight, S.L., and Russell, D.W. 1997. Endothelial PAS domain protein 1 (EPAS1), a transcription factor selectively expressed in endothelial cells. *Genes Dev.* **11**:72–82.
8. Gu, Y.Z., Moran, S.M., Hogenesch, J.B., Wartman, L., and Bradfield, C.A. 1998. Molecular characterization and chromosomal localization of a third α-class hypoxia inducible factor subunit, HIF3α. *Gene Expr.* **7**:205–213.
9. Burke, B., et al. 2002. Expression of HIF-1α by human macrophages: implications for the use of macrophages in hypoxia-regulated cancer gene therapy. *J. Pathol.* **196**:204–212.
10. Hollander, A.P., Corke, K.P., Freemont, A.J., and Lewis, C.E. 2001. Expression of hypoxia-inducible factor 1α by macrophages in the rheumatoid synovium: implications for targeting of therapeutic genes to the inflamed joint. *Arthritis Rheum.* **44**:1540–1544.
11. Cramer, T., et al. 2003. HIF-1α is essential for myeloid cell-mediated inflammation. *Cell.* **112**:645–657.
12. Schwartz, R.H., Gerber, M.A., and McCoy, P. 1985. Effect of atmosphere of incubation on the isolation of group A streptococci from throat cultures. *J. Lab. Clin. Med.* **106**:88–92.
13. Warnecke, C., et al. 2003. Activation of the hypoxia-inducible factor-pathway and stimulation of angiogenesis by application of prolyl hydroxylase inhibitors. *FASEB J.* **17**:1186–1188.
14. Kong, T., Eltzschig, H.K., Karhausen, J., Colgan, S.P., and Shelley, C.S. 2004. Leukocyte adhesion during hypoxia is mediated by HIF-1-dependent induction of β2 integrin gene expression. *Proc. Natl. Acad. Sci. U. S. A.* **101**:10440–10445.
15. Reeves, E.P., et al. 2002. Killing activity of

neutrophils is mediated through activation of proteases by K+ flux. *Nature.* **416**:291–297.
16. Guyonnet, V., Johnson, J.K., Bangalore, N., Travis, J., and Long, P.L. 1991. In vitro activity of the human neutrophil cathepsin G on Eimeria tenella sporozoites. *J. Parasitol.* **77**:775–779.
17. Miyasaki, K.T., and Bodeau, A.L. 1991. In vitro killing of oral *Capnocytophaga* by granule fractions of human neutrophils is associated with cathepsin G activity. *J. Clin. Invest.* **87**:1585–1593.
18. Shafer, W.M., and Onunka, V.C. 1989. Mechanism of staphylococcal resistance to non-oxidative antimicrobial action of neutrophils: importance of pH and ionic strength in determining the bactericidal action of cathepsin G. *J. Gen. Microbiol.* **135**:825–830.
19. Barrett, A.J. 1981. Cathepsin G. *Methods Enzymol.* **80**:561–565.
20. Cole, A.M., et al. 2001. Inhibition of neutrophil elastase prevents cathelicidin activation and impairs clearance of bacteria from wounds. *Blood.* **97**:297–304.
21. Sorensen, O.E., et al. 2001. Human cathelicidin, hCAP-18, is processed to the antimicrobial peptide LL-37 by extracellular cleavage with proteinase 3. *Blood.* **97**:3951–3959.
22. Nizet, V., and Gallo, R.L. 2003. Cathelicidins and innate defense against invasive bacterial infection. *Scand. J. Infect. Dis.* **35**:670–676.
23. Panyutich, A., Shi, J., Boutz, P.L., Zhao, C., and Ganz, T. 1997. Porcine polymorphonuclear leukocytes generate extracellular microbicidal activity by elastase-mediated activation of secreted proprotegrins. *Infect. Immun.* **65**:978–985.
24. Nizet, V., et al. 2001. Innate antimicrobial peptide protects the skin from invasive bacterial infection. *Nature.* **414**:454–457.
25. Lirk, P., Hoffmann, G., and Rieder, J. 2002. Inducible nitric oxide synthase–time for reappraisal. *Curr. Drug Targets Inflamm. Allergy.* **1**:89–108.
26. Gyurko, R., et al. 2003. Mice lacking inducible nitric oxide synthase demonstrate impaired killing of Porphyromonas gingivalis. *Infect. Immun.* **71**:4917–4924.
27. Alam, M.S., et al. 2002. Role of nitric oxide in host defense in murine salmonellosis as a function of its antibacterial and antiapoptotic activities. *Infect. Immun.* **70**:3130–3142.
28. Melillo, G., et al. 1997. Functional requirement of the hypoxia-responsive element in the activation of the inducible nitric oxide synthase promoter by the iron chelator desferrioxamine. *J. Biol. Chem.* **272**:12236–12243.
29. Jung, F., Palmer, L.A., Zhou, N., and Johns, R.A. 2000. Hypoxic regulation of inducible nitric oxide synthase via hypoxia inducible factor-1 in cardiac myocytes. *Circ. Res.* **86**:319–325.
30. Hu, R., Dai, A., and Tan, S. 2002. Hypoxia-inducible factor 1α upregulates the expression of inducible nitric oxide synthase gene in pulmonary arteries of hypoxic rat. *Chin. Med. J.* **115**:1833–1837.
31. Thornton, R.D., et al. 2000. Interleukin 1 induces hypoxia-inducible factor 1 in human gingival and synovial fibroblasts. *Biochem. J.* **350**:307–312.
32. Hellwig-Burgel, T., Rutkowski, K., Metzen, E., Fandrey, J., and Jelkmann, W. 1999. Interleukin-1β and tumor necrosis factor-α stimulate DNA binding of hypoxia-inducible factor-1. *Blood.* **94**:1561–1567.
33. Sandau, K.B., Fandrey, J., and Brune, B. 2001. Accumulation of HIF-1α under the influence of nitric oxide. *Blood.* **97**:1009–1015.
34. Zhou, J., Fandrey, J., Schumann, J., Tiegs, G., and Brune, B. 2003. NO and TNF-alpha released from activated macrophages stabilize HIF-1alpha in resting tubular LLC-PK1 cells. *Am. J. Physiol. Cell Physiol.* **284**:C439–C446.
35. Zhou, J., Schmid, T., and Brune, B. 2003. Tumor necrosis factor-alpha causes accumulation of a ubiquitinated form of hypoxia inducible factor-1α through a nuclear factor-kappaB-dependent pathway. *Mol. Biol. Cell.* **14**:2216–2225.
36. Kasuno, K., et al. 2004. Nitric oxide induces hypoxia-inducible factor 1 activation that is dependent on MAPK and phosphatidylinositol 3-kinase signaling. *J. Biol. Chem.* **279**:2550–2558.
37. Chan, A.T., Cleeve, V., and Daymond, T.J. 2002. Necrotising fasciitis in a patient receiving infliximab for rheumatoid arthritis. *Postgrad. Med. J.* **78**:47–48.
38. Nemoto, Y., et al. 1999. Differential effects of interleukin-4 and interleukin-10 on nitric oxide production by murine macrophages. *Inflamm. Res.* **48**:643–650.
39. Drapier, J.C., Wietzerbin, J., and Hibbs, J.B., Jr. 1988. Interferon-gamma and tumor necrosis factor induce the L-arginine-dependent cytotoxic effector mechanism in murine macrophages. *Eur. J. Immunol.* **18**:1587–1592.
40. Corradin, S.B., et al. 1993. Induction of macrophage nitric oxide production by interferon-gamma and tumor necrosis factor-alpha is enhanced by interleukin-10. *Eur. J. Immunol.* **23**:2045–2048.
41. Eigler, A., Moeller, J., and Endres, S. 1995. Exogenous and endogenous nitric oxide attenuates tumor necrosis factor synthesis in the murine macrophage cell line RAW 264.7. *J. Immunol.* **154**:4048–4054.
42. Marcinkiewicz, J., Grabowska, A., and Chain, B. 1995. Nitric oxide up-regulates the release of inflammatory mediators by mouse macrophages. *Eur. J. Immunol.* **25**:947–951.
43. Kuo, H.P., et al. 2000. Nitric oxide modulates interleukin-1beta and tumor necrosis factor-alpha synthesis by alveolar macrophages in pulmonary tuberculosis. *Am. J. Respir. Crit. Care Med.* **161**:192–199.
44. Iuvone, T., D'Acquisto, F., Carnuccio, R., and Di Rosa, M. 1996. Nitric oxide inhibits LPS-induced tumor necrosis factor synthesis in vitro and in vivo. *Life Sci.* **59**:PL207–PL211.
45. Wu, C.H., et al. 2003. Nitric oxide modulates pro- and anti-inflammatory cytokines in lipopolysaccharide-activated macrophages. *J. Trauma.* **55**:540–545.
46. Griffiths, L., et al. 2000. The macrophage - a novel system to deliver gene therapy to pathological hypoxia. *Gene Ther.* **7**:255–262.
47. Talks, K.L., et al. 2000. The expression and distribution of the hypoxia-inducible factors HIF-1α and HIF-2α in normal human tissues, cancers, and tumor-associated macrophages. *Am. J. Pathol.* **157**:411–421.
48. Nathan, C. 2003. Immunology: oxygen and the inflammatory cell. *Nature.* **422**:675–676.
49. Strieter, R.M. 2003. Mastering innate immunity. *Nat. Med.* **9**:512–513.
50. Clausen, B.E., Burkhardt, C., Reith, W., Renkawitz, R., and Forster, I. 1999. Conditional gene targeting in macrophages and granulocytes using LysMcre mice. *Transgenic Res.* **8**:265–277.
51. Walmsley, S.R., et al. 2005. Hypoxia-induced neutrophil survival is mediated by HIF-1α-dependent NF-κB activity. *J. Exp. Med.* **201**:105–115.
52. Kansal, R.G., McGeer, A., Low, D.E., Norrby-Teglund, A., and Kotb, M. 2000. Inverse relation between disease severity and expression of the streptococcal cysteine protease, SpeB, among clonal M1T1 isolates recovered from invasive group A streptococcal infection cases. *Infect. Immun.* **68**:6362–6369.
53. Liu, G.Y., et al. 2004. Sword and shield: linked group B streptococcal β-hemolysin/cytolysin and carotenoid pigment function to subvert host phagocyte defense. *Proc. Natl. Acad. Sci. U. S. A.* **101**:14491–14496.
54. Humar, D., et al. 2002. Streptolysin S and necrotising infections produced by group G streptococcus. *Lancet.* **359**:124–129.
55. Grunstein, J., Roberts, W.G., Mathieu-Costello, O., Hanahan, D., and Johnson, R.S. 1999. Tumor-derived expression of vascular endothelial growth factor is a critical factor in tumor expansion and vascular function. *Cancer Res.* **59**:1592–1598.
56. Blouw, B., et al. 2003. The hypoxic response of tumors is dependent on their microenvironment. *Cancer Cell.* **4**:133–146.